



HAL
open science

Challenging the [Ru(bpy) 3] 2+ Photosensitizer with a Triazatriangulenium Robust Organic Dye for Visible-Light-Driven Hydrogen Production in Water

Robin Gueret, Laurélie Poulard, Matthew Oshinowo, Jérôme Chauvin, Mustapha Dahmane, Grégory Dupeyre, Philippe P Lainé, Jérôme Fortage, Marie-Noëlle Collomb

► To cite this version:

Robin Gueret, Laurélie Poulard, Matthew Oshinowo, Jérôme Chauvin, Mustapha Dahmane, et al.. Challenging the [Ru(bpy) 3] 2+ Photosensitizer with a Triazatriangulenium Robust Organic Dye for Visible-Light-Driven Hydrogen Production in Water. ACS Catalysis, 2018, 8 (5), pp.3792-3802. 10.1021/acscatal.7b04000 . hal-04270803

HAL Id: hal-04270803

<https://u-paris.hal.science/hal-04270803v1>

Submitted on 5 Nov 2023

HAL is a multi-disciplinary open access archive for the deposit and dissemination of scientific research documents, whether they are published or not. The documents may come from teaching and research institutions in France or abroad, or from public or private research centers.

L'archive ouverte pluridisciplinaire **HAL**, est destinée au dépôt et à la diffusion de documents scientifiques de niveau recherche, publiés ou non, émanant des établissements d'enseignement et de recherche français ou étrangers, des laboratoires publics ou privés.

Challenging the $[\text{Ru}(\text{bpy})_3]^{2+}$ photosensitizer with a triazatriangulenium robust organic dye for visible light-driven hydrogen production in water

Robin Gueret,[†] Laurélie Poulard,[‡] Matthew Oshinowo,[†] Jérôme Chauvin,[†] Mustapha Dahmane,[‡] Grégory Dupeyre,[‡] Philippe P. Lainé,^{*,‡} Jérôme Fortage,^{*,†} and Marie-Noëlle Collomb^{*,†}

[†]Univ. Grenoble Alpes, CNRS, DCM, F-38000 Grenoble, France

[‡]Univ Paris Diderot, Sorbonne Paris Cité, ITODYS, UMR CNRS 7086, 15 rue J-A de Baïf, 75013 Paris, France

ABSTRACT: Photosensitizers used in homogeneous photocatalytic systems for artificial photosynthesis such as hydrogen production are typically based on expensive transition metal complexes such as d^6 ruthenium(II) or iridium(III). In this work, we demonstrate efficient H_2 production in acidic water by using an organic dye derived from the triazatriangulenium (**TATA**⁺) family as a visible-light-absorbing photosensitizer (PS). By associating the hydrosoluble tris(ethoxyethanol)triazatriangulenium with an efficient H_2 -evolving cobalt catalyst and ascorbic acid as sacrificial electron donor (SD), remarkable photocatalytic performances were reached in aqueous solution at pH 4.5, under visible light irradiation, with up to 8950 catalytic cycles *versus* catalyst. Noteworthy, the performances of this dye largely exceed those of the benchmark Ru tris-bipyridine in the same experimental conditions, when low concentrations of catalyst are used. This higher efficiency has been clearly ascribed to the remarkable robustness of the reduced form of the organic dye, **TATA**[•]. Indeed, the combination of the planar structure of **TATA**⁺ together with the presence of the three electron-donating nitrogen atoms, promote the stabilization of **TATA**[•] by delocalization of the radical, thereby preventing its degradation in the course of photocatalysis. By contrast the reduced form of the Ru photosensitizer, $[\text{Ru}^{\text{II}}(\text{bpy})_2(\text{bpy}^{\bullet})]^+$ ("**Ru**[•]"), is much less stable. Nanosecond transient absorption experiments confirm the formation of **TATA**[•] in the course of the photocatalytic process in accordance with the mechanism initiated by the reductive quenching of the singlet excited state of **TATA**⁺ by ascorbate. The second electron transfer from **TATA**[•] to the catalyst has also been evidenced by this technique with the detection of the signature of the reduced Co(I) form of the catalyst. The present study establishes that certain organic dyes are to be considered as relevant alternatives to expensive metal-based PSs insofar as they can exhibit a high stability under prolonged irradiation, even in acidic water, thereby providing valuable insights for the development of robust molecular systems only based on earth-abundant elements for solar fuel generation.

KEYWORDS : photosensitizer • triangulenium • hydrogen • photocatalysis • cobalt

1. INTRODUCTION

The conversion of solar energy into fuel molecules, such as dihydrogen by light-driven water-splitting is the subject of considerable interest as it constitutes a sustainable and carbon-neutral way to face current energy challenges.^{1,2} A largely investigated approach to reduce protons into H_2 , the reduction product of the water-splitting reaction, relies on molecular photocatalytic systems in homogeneous solution, which typically associate a light-harvesting photosensitizer (PS), a H_2 -evolving catalyst (Cat), and a sacrificial electron donor (SD) as the primary source of electrons.³⁻⁶ In such systems, the reductive quenching of the excited state of PS (PS*) generally occurs, leading to its reduced state (PS^{•-}), owing to the much higher concentration of SD than that of the catalyst. The PS^{•-} reduces, in its turn, the catalyst, which can then react with protons (or water) to produce H_2 . Another promising approach, more recently explored, is to immobilize the molecular photosensitizer and catalyst onto the surface of semi-conductor nanoparticles (SC), leading to semi-heterogeneous systems.⁷⁻¹¹ H_2 -evolving photocathodes have

been also constructed by immobilization of PS and Cat on a bulk SC,^{12,13} in view to be implemented in devices for water splitting, without requirement of sacrificial reagents. However, to fully satisfy the criteria of the sustainable H_2 production *via* water-splitting, these homogeneous or heterogeneous systems should not only involve earth-abundant elements but should also be stable and efficiently operative in water, without addition of toxic organic co-solvent(s). Much progress has been achieved in recent years in developing H_2 -evolving molecular catalysts that fulfill these requirements with the use of Co, Fe, Ni and Mo transition metal complexes.^{4,14-19} It remains nonetheless that most of the studies reported so far on this topic rely on the use of rare and expensive metal-based PS such as ruthenium ($[\text{Ru}(\text{bpy})_3]^{2+}$, denoted **Ru**; bpy = bipyridine), or iridium ($[\text{Ir}(\text{bpy})(\text{ppy})_2]^+$, denoted **Ir**; ppy = phenylpyridine) complexes and their derivatives. Indeed, these latter have the great asset of displaying both long-lived metal-to-ligand charge transfer (MLCT) excited states and very negative reduction potentials.²⁰ However, these inorganic PSs suffer from instability, in particular in water, insofar as their reduced states (ligand-centered radical anions) generated

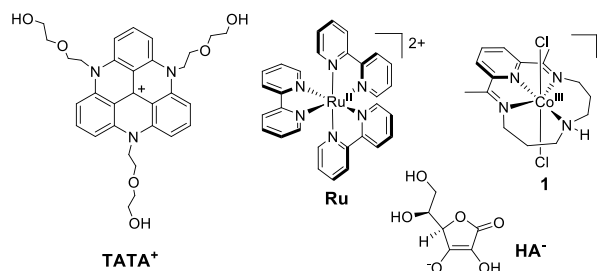
by the reductive quenching, can undergo either ligand(s) substitution or hydrogenation.²¹⁻²³

Metal-free organic dyes, only made of earth-abundant elements, constitute a very attractive alternative to these inorganic complexes,^{3,24} although they usually exhibit excited states of shorter lifetimes and less negative reduction potentials, compared to those of the **Ru** and **Ir** compounds. Since 2009, only a few families of commercially available organic dyes such as xanthenes,^{3,4,25-36} rhodamines³⁷ and acriflavine³⁸ and even more recently, synthetic dyes like BODIPY,³⁹⁻⁴³ perylene monoimides,^{44,45} and fluorenes⁴⁶ have been successfully employed in association with earth-abundant H₂-evolving catalysts in homogeneous photocatalytic systems. There have also been a few studies on the use of free-base porphyrins.⁴⁷ Typically, the poor stability of the reduced radical forms of these organic dyes, generated by reductive quenching, leads either to hydrogenation of their skeletons or to their dehalogenation (in the case of xanthenes). In other words, most of these dyes deteriorate quite readily during the photocatalytic processes, especially in acidic media. Because of the low stability and/or solubility of these sensitizers in aqueous solutions, these studies are generally conducted in mixed aqueous-organic solvents (e.g. CH₃CN/H₂O). Only the photocatalytic system with the perylene dye operates in acidic water (pH 4.0).^{44,45} However, this amphiphile chromophore forms hydrogels in water as a result of its supramolecular self-assembly, which limits the number of catalytic cycles per catalyst (turnovers, TONs), as in this instance of the water-soluble form of the Dubois' "Ni phosphine" catalyst (TON ≤ 400). Therefore, to access robust molecular homogeneous photocatalytic systems for hydrogen production made up of earth-abundant elements, one current challenge is to explore new families of organic dyes that will ideally combine: i) a high stability of their reduced forms, even in acidic water, ii) suitable electronic absorption and photophysical features, together with iii) suitable electrochemical properties at the fundamental and excited state to allow efficient electron transfer at the fundamental or excited state to the SD and the catalyst, as for instance sufficiently negative reduction potentials to reduce the H₂-evolving catalysts. In the case of the semi-heterogeneous and heterogeneous systems mentioned above, an efficient injection of holes or electrons from the excited state of the photosensitizer into the valence or conduction band of the semi-conductor would be also required.^{10,48}

Herein we introduce an organic dye derived from the triazatriangulenium carbocationic scaffold, **TATA**⁺, and its use as a visible-light-absorbing photosensitizer in a photocatalytic system designed for H₂ production. Triazatriangulenium dyes, first isolated in 2000 by Laursen and Krebs,^{49,50} are highly stable carbenium species that belong to the cationic triangulenes.^{51,52} Yet, to the best of our knowledge, such derivatives have never been used in photo-induced electron transfer reactions to drive catalytic processes. With the view to conducting photocatalysis in fully aqueous solution, we have synthesized a new water soluble **TATA**⁺ derivative that bears one ethoxyethanol chain per bridging nitrogen atom (Scheme 1, **TATA**⁺). This dye was tested in association with the cobalt tetraazamacrocyclic complex, [Co^{III}(CR14)Cl₂]⁺ (**1**), which is one of the most efficient H₂-evolving catalyst in acidic water,⁵³⁻⁵⁶ and ascorbate (HA⁻) as

SD (Scheme 1). With this system, in a fully aqueous solution at pH 4.5, outstanding photocatalytic performances for H₂ evolution both in terms of activity and stability have been achieved under visible light irradiation. Comparative studies in similar experimental conditions also showed that this organic PS displays performances by far exceeding those of benchmark [Ru(bpy)₃]²⁺ (denoted **Ru**) when low catalyst concentrations versus PS are used. The higher stability of the photocatalytic system with **TATA**⁺ is attributed to the higher stability of the photosensitizer in its reduced form, **TATA**[•], in acidic water compared to the reduced form of **Ru**, [Ru^{II}(bpy)₂(bpy^{•-})]⁺ (denoted **Ru**[•]).

Scheme 1. Photosensitizers, sacrificial donor and catalyst studied in this work.



The excellent stability of **TATA**[•] has been demonstrated by spectro-electrochemical studies, which have allowed obtaining its spectroscopic signature for the first time. Time resolved luminescence and nanosecond transient absorption spectroscopy were also employed to investigate the quenching kinetics of the **TATA**^{•*} excited state, as well as the related photocatalytic mechanism, thanks to the detection of key intermediates such as **TATA**[•] and the active Co(I) reduced form of the catalyst.

2. RESULTS AND DISCUSSION

2.1. Synthesis, spectroscopic and photophysical properties of **TATA**⁺.

The tris-ethoxyethanol-substituted **TATA**⁺ was synthesized in two steps from cheap reagents and isolated either as a chloride salt (after anion metathesis) to further increase its solubility in water for photocatalytic experiments (see below) or as its hexafluorophosphate (PF₆⁻) salt to perform spectro-electrochemical studies in CH₃CN (see SI and Figures S1-S10). The electronic absorption spectrum of **TATA**(PF₆) in CH₃CN is dominated by a broad absorption band in the visible domain spanning from 425 to 590 nm ($\lambda_{\text{max}} = 525$ nm; $\epsilon = 11,900$ M⁻¹ cm⁻¹; Figure 1A).^{52,57-59} The photocatalysis experiments are carried out in buffered aqueous media. It is thus important to obtain spectroscopic and photophysical characteristics of **TATA**⁺ in this solvent, all the more as, to the best of our knowledge, such studies have not yet been described in literature. In water, the shape of the visible band of **TATA**(Cl) is quite similar to that obtained for **TATA**(PF₆) in CH₃CN, with a large band in the visible region displaying two maxima at respectively 500 and 530 nm. The main difference lies in molar absorptivity, which is somewhat lower in water than that measured in CH₃CN ($\lambda_{\text{max}} = 530$ nm; ϵ

= 8800 M⁻¹ cm⁻¹; Figure 1B). The emission spectrum of **TATA**⁺ in aqueous solution at 298 K exhibits a maximum at 578 nm, close to the λ_{max} of the absorption spectrum (Stokes shift of about 50 nm), typical of a singlet excited state (Figure 1B). In water, at pH 4.5, the lifetime of **TATA**²⁺ was measured to be 14 ns, which is relatively long for the singlet excited state of an organic dye. Nevertheless, these results are consistent with those obtained in organic solvents for analogous *N*-alkyl **TATA**²⁺ derivatives ($\tau \approx 9$ ns and λ_{em} ranging from 548 to 568 nm).^{58,60} The small bathochromic shift of the λ_{em} as well as the increased τ measured for **TATA**²⁺ in water can be reasonably attributed to solvent change. From the absorption and emission spectra, we can estimate the energy value of the excited state (E_{0-0}) to be 2.23 eV, a value slightly higher than that of **Ru** (2.1 eV) (Table S1).

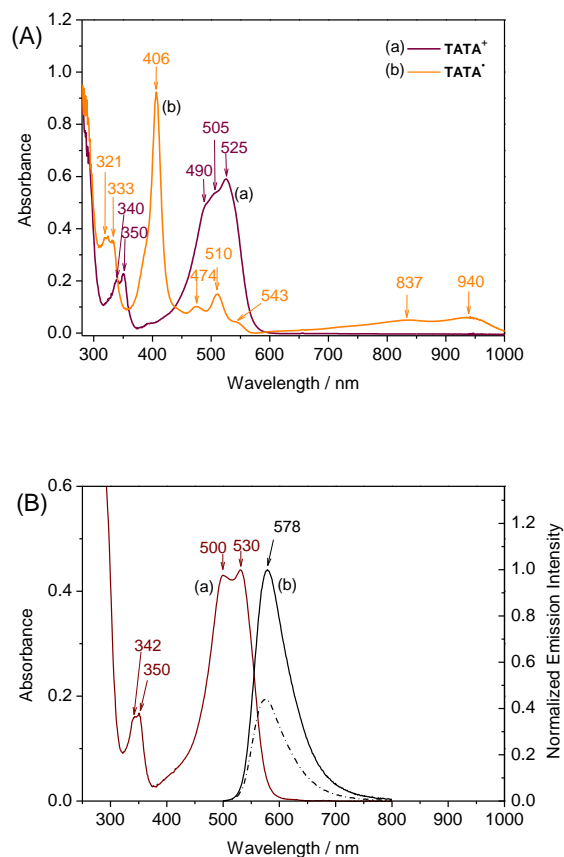


Figure 1. (A) UV-visible absorption spectra of a 0.5 mM solution of **TATA**(PF₆) in CH₃CN + 0.1 M [Bu₄N]BF₄ (a) before and (b) after an exhaustive reduction at -1.60 V vs Ag/AgNO₃ (formation of **TATA**[•]), optical path = 1 mm. (B) (a) UV-visible absorption spectrum of a 0.5 mM solution of **TATA**(Cl) and (b) normalized emission spectra ($\lambda_{\text{ex}} = 470$ nm) of a 10 μ M solution of **TATA**(Cl) under argon (full line) and under oxygen (dashed line) in an aqueous acetate buffer (1M) at pH 4.5.

Otherwise, the luminescence of **TATA**²⁺ is quenched at 56% in presence of O₂ in water (Figure 1B). Indeed, a recent study on structural analogues of **TATA**⁺, the azadioxatriangulenium (ADOTA) and diazoxatriangulenium (DAOTA),⁶¹ reveals

that the singlet excited state of these organic dyes with relatively long lifetime ($\tau \approx 20$ ns) can be also quenched by O₂. Other previous studies on other organic dye families such as anthracene and carboline reported similar quenching, debunking the classic rule where only triplet state are quenched by molecular oxygen.⁶²

Although in water the lifetime of the lowest excited state of **TATA**²⁺ is significantly shorter than that of **Ru**, which is a triplet MLCT (592 ns),⁵⁵ it should be long enough to allow bimolecular electron transfer reactions in homogeneous solutions. Singlet excited state lifetimes of the organic dyes already employed in homogeneous photocatalytic systems for H₂ production are shorter than 5 ns,^{25,41,44,45,63,64} which is in principle not sufficient to allow intermolecular electron transfer. However, it has been shown that the presence of heavy atoms as substituents (e. g. of halogen type) in fluorescein derivatives (*i. e.* Rose Bengal, Eosin, Erythrosin)^{25,29,30,65-71} and in BODIPY derivatives,^{72,73} facilitated intersystem crossing (ISC) between the initially-formed singlet excited state and the long-lived triplet excited state of lowest energy, from which intermolecular photoinduced electron transfer can occur. In the same time, the halogen substituents also contribute to the decomposition of the dyes *via* cleavage of the C-halogen bonds in their reduced forms. The production of H₂ with the non halogenated fluorescein has been nevertheless observed when this organic dye is used in high concentration, which leads to its aggregation and longer lived dimer emission when compared to diluted solutions ($\tau = 12$ vs 5 ns).^{25,27,31,33-36,74-78} Such an aggregation has not been observed with **TATA**⁺ in water since the λ_{max} of the visible bands and the associated molar absorption coefficients have been found to be independent from the concentration in the 10 μ M - 2 mM range (Figure S11).

2.2. Electrochemical properties of **TATA⁺: generation and characterization of **TATA**[•].** In agreement with compounds of this family,^{51,59,79-81} the cyclic voltammogram of **TATA**(PF₆) in CH₃CN displays a one-electron reversible reduction process at $E_{1/2} = -1.48$ V vs Ag/AgNO₃ (*i. e.* -1.59 V vs Fc^{+/0} or -1.18 V vs SCE) assigned to the redox couple “**TATA**^{+/•}”, followed by an irreversible wave, assigned to “**TATA**^{•/2+}” ($E_{\text{pc}} = -2.10$ V vs Ag/AgNO₃, see Figures 2A and S12, and Table S1). Four successive one-electron oxidation waves are also recorded ($E_{\text{pa}} = +0.96$, $+1.38$, $+1.68$ and $+2.14$ V) with the first one, quasi-reversible, assigned to the formation of the radical dication **TATA**²⁺ (Figure 2). The very negative potential of the first reduction wave of this organic dye ($E_{1/2} = -1.18$ V vs SCE) will allow an efficient reduction of the cobalt catalyst **1** ($E_{1/2} = -0.85$ V vs SCE in water for the Co^{II/Co}I couple) by the photo-generated reduced radical form, **TATA**[•] (Table S1).^{53,55} Although this reduction potential is less negative than that of **Ru** by about 160 mV (potentials comparison in CH₃CN, Table S1), it is more negative than most of the dyes already tested in H₂ evolving photocatalytic systems (around -1.0 V in CH₃CN). Only non halogenated BODIPY^{39-43,82} and fluorescein^{3,67} present reduction potentials in the $-1.16/-1.25$ V range vs SCE (in CH₃CN), similar to that of **TATA**⁺.

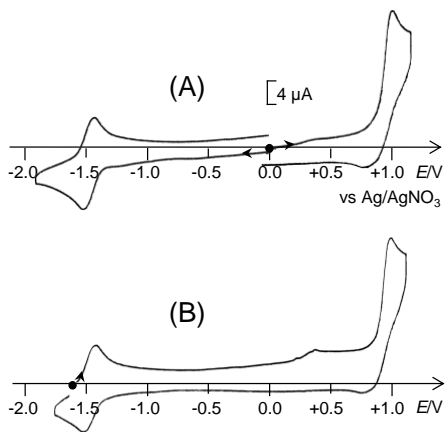


Figure 2. Cyclic voltammograms at a glassy carbon electrode (scan rate = 0.1 V s^{-1}) of 0.5 mM solution of $\text{TATA}(\text{PF}_6)$ in $\text{CH}_3\text{CN} + 0.1 \text{ M}$ $[\text{Bu}_4\text{N}]\text{BF}_4$: (A) initial solution and (B) after an exhaustive reduction at $-1.60 \text{ V vs Ag/AgNO}_3$ leading to the quantitative formation of TATA^\bullet (after transfer of one electron per molecule of initial TATA^+).

The high stability of the reduced radical form of the PS is also a key factor for the long term durability and thus, for the efficiency of photocatalytic systems for H_2 production involving a reductive pathway. As stated in the introduction, the commonly employed visible-light photosensitizers are polypyridyl transition metal complexes and organic molecules that are, however, limited by the instability of their reduced forms. The stability of TATA^\bullet in CH_3CN was investigated by bulk electrolysis at $-1.60 \text{ V vs Ag/AgNO}_3$, at room temperature (Figure 1A). After the exchange of one-electron, TATA^\bullet is quantitatively formed as shown by the resulting cyclic voltammogram (Figures 2B and S12). Upon electrolysis, the visible bands of the initial bright reddish solution of TATA^+ gradually decrease while a new intense and sharp absorption band at 406 nm increases, along with growth of several less intense bands at both longer and shorter wavelengths (Figures 1A and S13). This spectroscopic signature of the TATA^\bullet derivative, obtained for the first time, has allowed the unambiguous identification of this species in the course of photocatalysis by transient absorption spectroscopy (see below). In addition, the electro-generated solution is perfectly stable for at least one hour under anaerobic conditions, thereby demonstrating the excellent stability of TATA^\bullet in CH_3CN . X-band EPR spectroscopy also confirms the formation of TATA^\bullet . Indeed, the X-band EPR signature of the reduced solution with a single isotropic signal centered at $g = 2.00$ is characteristic of an organic radical species,⁷⁹ fully consistent with the formation of TATA^\bullet (Figure S14). As expected, bulk electrolysis at -1.0 V is quantitatively restoring TATA^+ (Figure S12). This noticeable stability of TATA^\bullet can be accounted for its peculiar structure, namely a planar scaffold incorporating three electron-donating nitrogen atoms. This configuration is likely to promote delocalization of the radical. Open-shell species in which the radical is less delocalized as in the MLCT states of Ru photosensitizers are indeed much more reactive and potentially subject to dimerization or reaction with solvents.⁷⁹

2.1. Photocatalytic activities for hydrogen production with the $\text{TATA}^+/\text{1}/\text{HA}^-/\text{H}_2\text{A}$ system. We have investigated the photocatalytic H_2 production with TATA^+ as the PS using catalyst **1** in a 5 mL deaerated aqueous solution in presence of an acetate buffer solution (1.0 M) and $\text{HA}^-/\text{H}_2\text{A}$ (total concentration of 0.1 M) under visible light irradiation ($400 - 700 \text{ nm}$; see Tables S2 and S3). The amount of H_2 produced was quantified in real time by gas chromatography, and used to calculate the turnover number and the initial turnover frequency of catalyst, denoted TON_{Cat} and TOF_{Cat} , respectively (Table S4). All experiments were repeated at least three times and reproducible values (error margin of 4%) were obtained. Control experiments in absence of either $\text{HA}^-/\text{H}_2\text{A}$ or **1** did not produce any appreciable amounts of H_2 , whilst a very small production of H_2 was detected with TATA^+ and $\text{HA}^-/\text{H}_2\text{A}$. This amount, within the error margin, can be considered as negligible (Figure S16A and Table S4).

The pH dependence of the photocatalytic activity of $\text{TATA}^+/\text{1}/\text{HA}^-/\text{H}_2\text{A}$ was first evaluated with $500 \mu\text{M}$ of TATA^+ and $10 \mu\text{M}$ of **1** (Figure 3). Regardless of the pH, the system is very active with TON_{Cat} values that largely exceed 1000. The highest performances were obtained at pH 4.5, with a TON_{Cat} value of 4076 after 23.5 hours of irradiation, compared to about 3000 TON_{Cat} at pH 4.0 or 5.0. At pH 3.0 and 6.0, the activity is lower with about 1435 and 1700 TON_{Cat} , respectively. While the initial TOF values are quite similar for pH 3.0, 4.0 and 4.5, the stability of the photocatalytic system is significantly enhanced at pH 4.5, resulting in the highest TON_{Cat} values. Conversely, the initial TOF decreases significantly at pH higher than 4.5, with an induction period starting to appear. Such pH dependence results from a balance between several factors, such as the reactivity and the stability of the catalyst, as well as the efficiency of the photo-induced electron transfer process.^{5,83,84} Indeed, when the pH increases, the production of H_2 is limited by the disfavored protonation of the reduced form of the cobalt catalyst to generate the hydride catalytic intermediate. At more acidic pH, it is instead the formation of the reduced state of the photosensitizer which is disfavored because the concentration of the SD, HA^- , decreases.

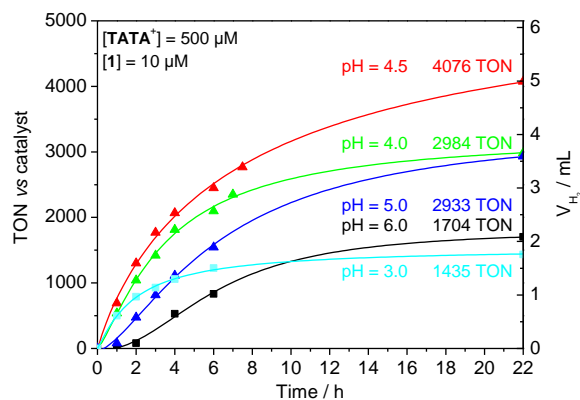


Figure 3. Photocatalytic hydrogen production (TON vs catalyst) as a function of time from a deaerated 1 M acetate buffer (5 mL) at different pH under $\lambda = 400 - 700 \text{ nm}$ irradiation in the presence

of TATA^+ (0.5 mM), $[\text{Co}(\text{CR14})\text{Cl}_2]\text{Cl}$ (**1**, 10 μM), and $\text{NaHA}/\text{H}_2\text{A}$ (0.1 M).

Thus, we further explored the photocatalytic activity of this system at pH 4.5. At this pH, mercury poisoning experiments allowed to ruling out the formation of cobalt colloids. Indeed, the presence of a large excess of mercury has no meaningful effect on the catalytic activity of the $\text{TATA}^+/\text{1}/\text{HA}^-/\text{H}_2\text{A}$ system (Figure S15), clearly indicating that no detectable quantity of colloid made of $\text{Co}(0)$ nanoparticles was formed during the process of photocatalytic H_2 production. This is in agreement with previous experiments using this catalyst in association with **Ru** as photosensitizer.⁵³ In addition if the cobalt catalyst **1** is replaced by a simple cobalt salt, $[\text{Co}(\text{OH}_2)_6]\text{Cl}_2$, the very small amount of H_2 corresponds to that produced by $\text{TATA}^+/\text{HA}^-/\text{H}_2\text{A}$ solutions (Table S4).

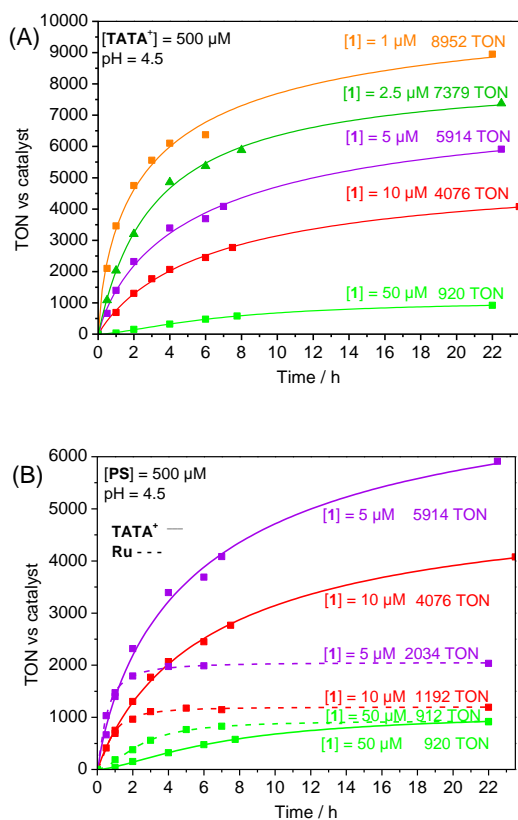


Figure 4. Photocatalytic hydrogen production (TON) as a function of time from a deaerated 1 M acetate buffer (5 mL) at pH 4.5 under visible light irradiation in presence of PS (0.5 mM), $\text{NaHA}/\text{H}_2\text{A}$ (0.1 M) and with various concentrations of **1**, (A) TATA^+ and (B) comparison of TATA^+ and **Ru**.

Then, the photocatalytic activity of $\text{TATA}^+/\text{1}/\text{HA}^-/\text{H}_2\text{A}$ was investigated by varying the concentration of **1**. When the concentration of **1** decreases from 50 to 1 μM (whilst maintaining TATA^+ at 500 μM), considerably higher TON_{Cat} and TOF_{Cat} values were obtained (e.g. TON_{Cat} from 920 up to 8952 corresponding to TOF_{Cat} values of 94 to 6500 h^{-1} ; see Figures 4A and S16A, Table S4). Such a behavior, generally observed with similar photocatalytic systems using other families of cobalt catalysts in water,⁸⁵⁻⁹⁴ is expected because

the increase of the PS/Cat ratio promotes the reduction of the catalyst, *i.e.* the reduction of the catalyst is less or not limited by the amount of PS in solution, leading to the formation of the hydride species as key intermediate for H_2 production. However, unlike what is observed here, decreasing the concentration of the catalyst usually leads to a significant decrease in the stability of the photocatalytic system. In addition, the TON_{Cat} values measured here with **1** are extremely high, much higher than those we previously obtained with this catalyst in association with **Ru** as the PS that never exceeds 2000. In fact, in our previous studies, the maximum TON_{Cat} values reached in water were 1100 at pH 4.0 with **Ru** (500 μM) and **1** (50 μM) and 1950 at pH 4.5 with **Ru** (500 μM) and **1** (1 μM).^{53,55} In these studies, although an identical experimental set-up was used, aqueous solutions were buffered with higher concentrations of $\text{HA}^-/\text{H}_2\text{A}$ (total concentration of 1.1 M) and this can affect the stability of the photocatalytic system.

To reliably compare the respective activities of the metal-free TATA^+ and **Ru** as the reference PS, we thus performed experiments with **Ru** in strictly identical conditions, *i.e.* in 1.0 M acetate buffer at pH 4.5 with 0.1 M $\text{HA}^-/\text{H}_2\text{A}$. A small quantity of H_2 was also detected in aqueous 1.0 M acetate buffer solutions containing only **Ru** (500 μM) and $\text{HA}^-/\text{H}_2\text{A}$ (0.1 M) (Figure S16B and Table S4), in agreement with previous observations.^{53,55,93,95} Interestingly, this amount is larger than that produced with TATA^+ in the same conditions by about four times (see above and Table S4). This is consistent with the fact that the reduced state of **Ru**, $[\text{Ru}^{\text{II}}(\text{bpy})_2(\text{bpy}^*)]^+$, “denoted **Ru**”, is a stronger reducing agent than TATA^+ by about 160 mV (Table S1). This amount of H_2 represents only about 3% at the highest tested catalyst concentration (50 μM), and about 10% at the lowest concentration (5 μM) (see below and Table S4 for corrected values denoted $\text{TON}_{\text{Cat}}^*$ and $\text{TOF}_{\text{Cat}}^*$).

Figure 4B shows the comparison of activities of both the PS at three different concentrations of **1**: 50, 10 and 5 μM . For lower concentrations in **1**, the results obtained with **Ru** were not reproducible enough due to the slight quantity of H_2 produced, which is close to the blank, *i.e.* **Ru** (500 μM) and $\text{HA}^-/\text{H}_2\text{A}$ (0.1 M). At the highest catalyst concentration of 50 μM , the H_2 production is similar for both PS around 22 h (about 900 TON_{Cat}), although the photocatalytic system with TATA^+ is still producing H_2 at this stage. By contrast, a significant difference between the two PSs appears at lower concentrations in catalyst, the catalytic activity with TATA^+ being much more effective. Indeed, at 10 and 5 μM , TON_{Cat} values of 4076 and 5914 were respectively measured for TATA^+ , to be compared with values of 1190 and 2034 for **Ru**. The markedly higher TON_{Cat} values obtained with TATA^+ as PS can be directly correlated to the higher stability of the photocatalytic system under prolonged visible-light irradiation. Indeed, with this organic dye, H_2 is produced for more than 22 h whatever the catalyst concentration compared to 3 – 6 h with **Ru**.

In fact, the organic dye TATA^+ was found to be by far more stable than **Ru** as PS under these photocatalytic conditions of acidic aqueous solutions, as shown by UV-vis absorption spectrophotometry. The remarkable stability of TATA^+ is

indeed supported by monitoring the UV/vis absorption spectra of 1.0 M acetate buffered solutions of **TATA**⁺ (500 μ M) with HA⁻/H₂A (0.1 M) at pH 4.5, either in the absence or presence of catalyst (Figures 5). In the absence of **1**, the spectrum remains almost unchanged even after a prolonged irradiation of 46 h.

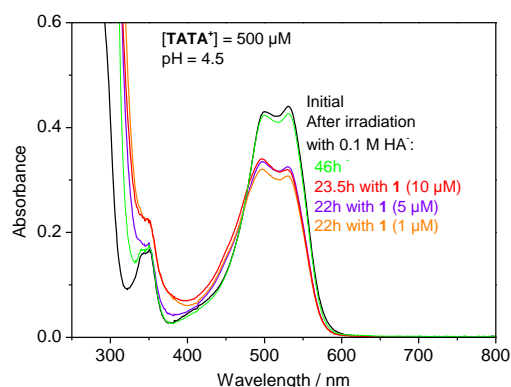


Figure 5. UV-visible absorption spectra of 0.5 mM **TATA**(Cl) in 1 M acetate buffer (5 mL) at pH 4.5 and NaHA/H₂A (0.1 M), after 46 h of visible irradiation without catalyst and after about 22h of irradiation with various concentrations of **1**. Optical path = 1 mm.

In similar conditions, in agreement with previous observations,⁸⁸ **Ru** is much less stable, since after only 3 h, the intensity of its visible band at 450 nm has already decreased by 40% (Figure S17A). This degradation is well-known to be the result of the poor stability of the reduced formed, **Ru**⁻, generated by the reductive quenching of the excited state of **Ru** (**Ru**^{*}) by HA⁻, which can undergo substitution of one of its bpy ligands in acidic aqueous solution by solvent molecules and/or anions such as ascorbate or acetate.^{85,88} Ruthenium bis-pyridine species also exhibit absorption bands in the visible domain with maxima close to that of **Ru**, but with ca. twofold smaller molecular absorption coefficients.^{88,96} **Ru** is thus fully transformed after about 22 h (Figure S17A). This degradation of **Ru** can be only partially limited in the presence of relatively high concentration in catalyst (~50 μ M) (Figure S17B) as this catalyst acts as a quencher of the **Ru**⁻ species (see below). In the case of **TATA**⁺, at least 75% of the initial concentration of the organic dye is saved after 22 – 23.5 h of irradiation in the presence of **1**, whatever its concentration (Figure 5). This behavior is fully consistent with the fact that the H₂ production is still maintained after 22 h, even at very low catalyst concentration (Figure 4A). Such a behavior is unusual since generally, as stated above, decreasing the catalyst concentration while maintaining constant the concentration of the PS, significantly decreases the stability of the photocatalytic system. The degradation of **TATA**⁺ therefore appears not to be the limiting factor for the H₂ production in this time scale. The progressive decrease in hydrogen production over time for the photocatalytic system with **TATA**⁺ is thus most likely the result of the partial catalyst degradation that can be also coupled to the accumulation of dehydroascorbic acid, which is the oxidation product of the ascorbate donor,^{5,86,88,91,97} rather than that of the degradation of the PS itself, that remains active after 22 h

(about 75 % of the initial amount of **TATA**⁺ is still present in solution (Figure 5)). Dehydroascorbic acid is known to be a good electron acceptor capable of preventing any electron transfer to the catalyst by trapping the electron from the reduced photosensitizer and thus short-circuiting the catalysis.^{86,91,97} Indeed, the addition of catalyst after 22 h of photocatalysis restores only partially the catalytic activity (about twenty percent) consistent with a large accumulation of dehydroascorbic acid at this stage (Figure S18).

2.2. Mechanistic insight into the **TATA**⁺/**1**/HA⁻/H₂A system from photophysical and transient absorption measurements.

We have investigated in greater details the first steps of the photocatalytic mechanism by carrying out photophysical studies. It should be first recalled that upon dissolution of the cobalt(III) catalyst **1** in an aqueous NaHA/H₂A buffer, the [Co^{II}(CR14)(OH₂)₂]²⁺ complex is immediately generated *in situ* via through the one-electron reduction of **1** by HA⁻, accompanied with the substitution of the chloride anions by water molecules.⁵³ The initial step of the photocatalytic cycle could either be a reductive quenching of the excited state of **TATA**⁺, denoted **TATA**^{*}, by electron transfer from HA⁻ that leads to the formation of **TATA**[•], or an oxidative quenching of **TATA**^{*} by the catalyst [Co^{II}(CR14)(OH₂)₂]²⁺, thereby generating the **TATA**²⁺ species and [Co^I(CR14)(OH₂)_x]⁺. In fact, at pH 4.5, the luminescence of **TATA**^{*} is quenched by HA⁻ with a rate constant k_{q1} of $3.6 \times 10^9 \text{ M}^{-1} \text{ s}^{-1}$ (Figure S19A), a value two orders of magnitude higher than those obtained between NaHA and **Ru**^{*} ($2 \times 10^7 \text{ M}^{-1} \text{ s}^{-1}$).⁹⁸ This difference can be explained by the greater driving force for the electron transfer between **TATA**^{*} and NaHA ($\Delta G^\circ = -0.95 \text{ eV}$) than between **Ru**^{*} and NaHA ($\Delta G^\circ = -0.49 \text{ eV}$). In the case of oxidative quenching of **TATA**^{*} by the [Co^{II}(CR14)(H₂O)₂]²⁺ catalyst, the quenching constant is 3.4-fold higher with a k_{q2} value of $1.23 \times 10^{10} \text{ M}^{-1} \text{ s}^{-1}$ (Figure S19B). This value, close to the limit of the diffusion kinetics of the species in solution, is further higher than that measured for the quenching of **Ru**^{*} by [Co^{II}(CR14)(H₂O)₂]²⁺.⁵³ Nevertheless, similarly to previous studies with **Ru**,^{55,93} because of the concentration of HA⁻ (0.076 M) by far higher than that of the cobalt catalyst (in the 1 – 50 μ M range) under the photocatalytic conditions, the reductive quenching by HA⁻ dominates with a pseudo-first order kinetics of $2.73 \times 10^8 \text{ s}^{-1}$ vs. $1.23 - 61.5 \times 10^4 \text{ s}^{-1}$ for the oxidative quenching by the cobalt catalyst.

Nanosecond transient absorption spectroscopy measurements further substantiated that the initial step of the photocatalytic cycle is the reductive quenching of **TATA**^{*} by HA⁻. Indeed the spectral signature of **TATA**[•] that is, the sharp absorption band at around 400 nm is detected in the transient absorption spectra obtained after irradiation of an aqueous solution containing **TATA**⁺ and HA⁻ with or without **1** (Figures 6 and 7, respectively). In the absence of **1**, the regeneration of **TATA**⁺ results in an intricate charge recombination process with various oxidized forms of ascorbate,⁹⁹ which can be fitted according to a second-order kinetics with a rate constant of $3.26 \times 10^9 \text{ M}^{-1} \text{ s}^{-1}$ (Figures S20-S21). In the presence of **1**, the decay of **TATA**[•] leading to **TATA**⁺ is significantly faster as a consequence of the electron transfer process with the Co(II) form of the catalyst leading to

its reduction into Co(I), which competes efficiently with the back electron transfer process between **TATA**[•] and the oxidized forms of HA⁻ (Figure 7 and S22). Indeed the decay at 400 nm is concomitant with an increase in absorbance of a large band at around 680 nm typical of the Co(I) reduced form of the catalyst (Figure 7).⁵⁵ The decay of **TATA**[•] in presence of [Co^{II}(CR14)(OH₂)₂]²⁺ can be fitted with a mono-exponential function yielding a pseudo first-order rate-constant of $1.47 \times 10^5 \text{ s}^{-1}$ (Figure S21).

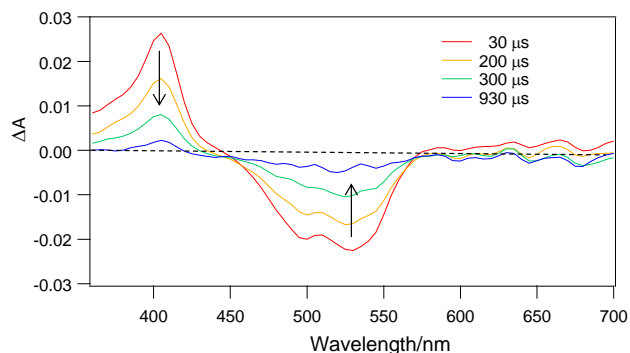


Figure 6. Transient absorption spectra after laser excitation at 532 nm of a deaerated 1 M aqueous acetate buffered solution at pH 4.5 containing **TATA**⁺ (100 μM) and NaHA/H₂A (0.1 M) within the 30-900 μs time range.

Taking into account the concentration of the catalyst (200 μM), the electron transfer reaction between **TATA**[•] and [Co^{II}(CR14)(OH₂)₂]²⁺ corresponds to a second order kinetics of $7.35 \times 10^8 \text{ M}^{-1} \text{ s}^{-1}$. This kinetics is around two times smaller than that between **Ru**⁻ and [Co^{II}(CR14)(OH₂)₂]²⁺ ($1.4 \times 10^9 \text{ M}^{-1} \text{ s}^{-1}$),⁵⁵ most likely because of the less exergonic (by 0.16 V) reaction occurring with **TATA**[•] (see Table S1).

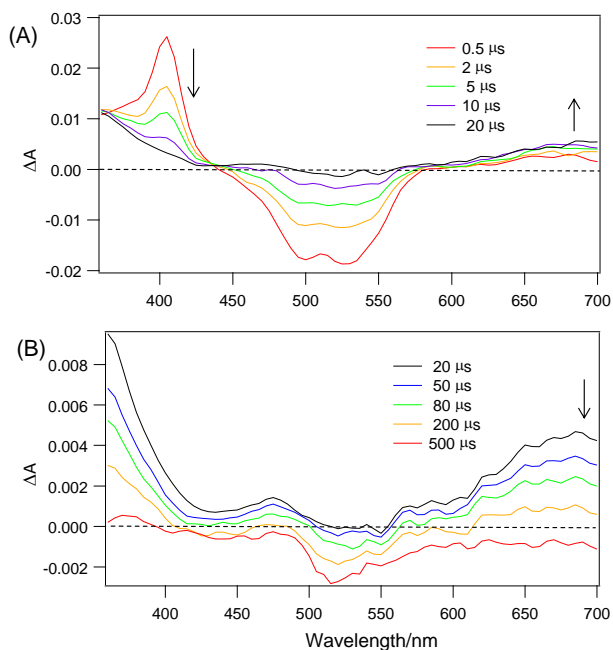


Figure 7. Transient absorption spectra recorded after laser excitation at 532 nm of a deaerated 1 M acetate buffer solution at pH 4.5 containing **TATA**⁺ (100 μM), NaHA/H₂A (0.1 M) and **1** (200 μM) (pathlength = 1 cm) within the 0.5 – 20 μs (A) or 20 – 500 μs (B) time ranges.

These experiments also highlight the appearance and decay of the absorbance at 680 nm of the reduced Co(I) form of the catalyst⁵⁵ stemming from an electron transfer from **TATA**[•] to [Co^{II}(CR14)(OH₂)₂]²⁺ (Figure 7). The decay of Co(I) with a rate constant of $7.1 \times 10^3 \text{ s}^{-1}$ (Figure S22) is assumed to be controlled by its protonation, leading to a hydride complex as intermediate species for H₂ generation.^{53,100} However, such hydride cobalt species are elusive species and thus difficult to observe experimentally¹⁰¹ in contrast to H₂-evolving catalysts based on polypyridinyl rhodium complexes for which hydride intermediates can be isolated and characterized.^{102,103}

The reductive quenching of positively charged photosensitizers by anionic electron donors has been shown to have a relevance to the formation of ion-pair between the cationic PS and the anionic SD.¹⁰⁴⁻¹⁰⁶ In such cases, the yield of charge-separated state used to saturate when the SD concentration increases. We did not observe such saturation behavior by transient absorption spectroscopy experiments upon increasing the HA⁻/H₂A concentration, but instead a decrease of the generation yield of the reduced species, **TATA**[•] (Figure S23). In addition, the absorption spectra of **TATA**[•] is not significantly affected by the HA⁻/H₂A concentration in the range of 5 mM to 1 M. These observations provide no evidences to support the formation of an ion-pair between **TATA**⁺ and HA⁻.

3. CONCLUSIONS

In summary, we introduced a new class of organic photosensitizer that belongs to the triazatriangulenium family for the visible-light driven H₂ production. The tris(ethoxyethanol)triazatriangulenium derivative (**TATA**⁺) has been established as an excellent photosensitizer when combined to a molecular H₂-evolving catalyst and ascorbate as a sacrificial electron donor in purely aqueous acidic solution. Indeed, the relatively long lifetime of its singlet excited state (14 ns), coupled to a negative reduction potential of -1.18 V vs SCE and to an excellent stability of its reduced form, the organic radical **TATA**[•], make this organic PS perfectly suited for photo-induced electron transfer reactions to drive catalytic processes, especially through a reductive quenching pathway. Very efficient H₂ production has been observed in water at pH 4.5 when this dye is associated with both a cobalt tetraazamacrocyclic catalyst (**1**) and ascorbate. In addition to the intrinsic efficiency of the cobalt complex as H₂-evolving catalyst in water, the high photocatalytic performances of this molecular system are due to its high stability over time, even at low catalyst concentration. This stability is directly correlated with the remarkable stability of **TATA**[•], generated by the reductive quenching, whose particular structure contributes to the delocalization of the radical, limiting its reactivity. It is worth highlighting that the performances of this dye can by far exceed those of the benchmark Ru tris-bipyridine in similar conditions as a consequence of the lower stability of its [Ru^{II}(bpy)₂(bpy^{•-})]⁺ form (denoted **Ru**⁻). The spectroscopic signature of **TATA**[•], obtained for the first time

from bulk electrolysis experiments, has unambiguously allowed identifying the formation of this species during the photocatalytic cycle by transient absorption spectroscopy. The key Co(I) intermediate species was also identified by this technique, thus supporting the subsequent electron transfer from **TATA**⁺ to the cobalt catalyst.

This study also demonstrates that the cobalt tetraazamacrocyclic catalyst is capable of achieving a large number of catalytic cycles, up to 8950 at 1 μM , if the system is not limited by the stability of the PS. It should be emphasized that the performances of the **TATA**⁺/I/HA⁻ system described in this work are also by far higher than those of the perylene/Ni phosphine/HA⁻ system, the only other molecular system with an organic dye already reported to operate in acidic aqueous solutions.

Finally, organic dyes belonging to the triazatriangulenium family, exhibiting sufficiently negative reduction potentials, could certainly be used with several other families of H₂-evolving molecular catalysts. These results more widely demonstrate that organic dyes can be considered as relevant and valuable alternatives to (noble) metal-based photosensitizers and thus pave the way towards robust homogeneous molecular photocatalytic systems in aqueous solutions, based on earth-abundant elements, not only for H₂ production but also for CO₂ reduction.

ASSOCIATED CONTENT

Supporting Information.

This material is available free of charge via the Internet at <http://pubs.acs.org>.

General experimental details, synthesis procedure of **TATA**⁺, NMR, mass spectra and cyclic voltammograms of **TATA**⁺ before and after electrolysis, redox potentials, UV-visible spectra of **TATA**⁺ during electrolysis, EPR spectrum of **TATA**⁺, general procedure for photocatalytic hydrogen generation, poisoning mercury experiments, photocatalytic H₂ production with **TATA**⁺ and **Ru** in function of nH₂ and vH₂, UV-visible spectra with **Ru** and ascorbate after irradiation in presence and absence of catalyst, transient absorption decay at 400 nm of **TATA**⁺ and ascorbate, and at 400 and 680 nm in presence of the catalyst (Figures S1-S20 and Tables S1-S4).

AUTHOR INFORMATION

Corresponding Author

*philippe.laine@univ-paris-diderot.fr

*jerome.fortage@univ-grenoble-alpes.fr

*marie-noelle.collomb@univ-grenoble-alpes.fr

ORCID

Jérôme Fortage : 0000-0003-2673-0610

Marie-Noëlle Collomb : 0000-0002-6641-771X

Funding Sources

LABEX ARCANE (ANR-11-LABX-0003-01); IDEX USPC;

MRES

Notes

The authors declare no conflict of interest.

ACKNOWLEDGMENT

R. G. and L. P. thank respectively the University of Grenoble Alpes and the MRES for their PhD grants. G. D. thanks the IDEX USPC for financial support. The authors thank for financial supports the LABEX ARCANE (ANR-11-LABX-0003-01) for the project H₂Photocat. The ICMG FR 2067 together with the COST CM1202 program (PERSPECT H₂O) as well as the interdisciplinary National Network for RPE TGE, which did allow the EPR measurements and facilities, together with the CNRS agency, which did support this work, are also thanked.

ABBREVIATIONS

PS, photosensitizer; Cat, H₂-evolving catalyst; SD, sacrificial electron donor; TATA, triazatriangulenium; H₂A, ascorbic acid; TON, turnover number.

REFERENCES

- (1) Esswein, A. J.; Nocera, D. G. *Chem. Rev.* **2007**, *107*, 4022-4047.
- (2) Berardi, S.; Drouet, S.; Francas, L.; Gimbert-Surinach, C.; Guttentag, M.; Richmond, C.; Stoll, T.; Llobet, A. *Chem. Soc. Rev.* **2014**, *43*, 7501-7519.
- (3) Eckenhoff, W. T.; Eisenberg, R. *Dalton Trans.* **2012**, *41*, 13004-13021.
- (4) Han, Z.; Eisenberg, R. *Acc. Chem. Res.* **2014**, *47*, 2537-2544.
- (5) Stoll, T.; Castillo, C. E.; Kayanuma, M.; Sandroni, M.; Daniel, C.; Odobel, F.; Fortage, J.; Collomb, M.-N. *Coord. Chem. Rev.* **2015**, *304-305*, 20-37.
- (6) Kowacs, T.; Pan, Q.; Lang, P.; O'Reilly, L.; Rau, S.; Browne, W. R.; Pryce, M. T.; Huijser, A.; Vos, J. G. *Faraday Discuss.* **2015**, *185*, 143-170.
- (7) Lakadamyali, F.; Reynal, A.; Kato, M.; Durrant, J. R.; Reisner, E. *Chem. Eur. J.* **2012**, *18*, 15464-15475.
- (8) Gross, M. A.; Reynal, A.; Durrant, J. R.; Reisner, E. *J. Am. Chem. Soc.* **2014**, *136*, 356-366.
- (9) Wang, M.; Han, K.; Zhang, S.; Sun, L. *Coord. Chem. Rev.* **2015**, *287*, 1-14.
- (10) Willkomm, J.; Orchard, K. L.; Reynal, A.; Pastor, E.; Durrant, J. R.; Reisner, E. *Chem. Soc. Rev.* **2016**, *45*, 9-23.
- (11) Warnan, J.; Willkomm, J.; Ng, J. N.; Godin, R.; Prantl, S.; Durrant, J. R.; Reisner, E. *Chem. Sci.* **2017**, *8*, 3070-3079.
- (12) Yu, Z.; Li, F.; Sun, L. *Energy Environ. Sci.* **2015**, *8*, 760-775.
- (13) Queyriaux, N.; Kaeffer, N.; Morozan, A.; Chavarot-Kerlidou, M.; Artero, V. *J. Photochem. Photobiol. C, Photochem. Rev.* **2015**, *25*, 90-105.
- (14) Losse, S.; Vos, J. G.; Rau, S. *Coord. Chem. Rev.* **2010**, *254*, 2492-2504.
- (15) Wang, M.; Chen, L.; Sun, L. *C. Energy Environ. Sci.* **2012**, *5*, 6763-6778.
- (16) Queyriaux, N.; Jane, R. T.; Massin, J.; Artero, V.; Chavarot-Kerlidou, M. *Coord. Chem. Rev.* **2015**, *304*, 3-19.
- (17) Du, P.; Eisenberg, R. *Energy Environ. Sci.* **2012**, *5*, 6012-6021.
- (18) Koshiba, K.; Yamauchi, K.; Sakai, K. *Angew. Chem., Int. Ed. Engl.* **2017**, *56*, 4247-4251.
- (19) Eckenhoff, W. T. *Coord. Chem. Rev.*, <https://doi.org/10.1016/j.ccr.2017.11.002>.
- (20) Yuan, Y.-J.; Yu, Z.-T.; Chen, D.-Q.; Zou, Z.-G. *Chem. Soc. Rev.* **2017**, *46*, 603-631.
- (21) Khnayzer, R. S.; McCusker, C. E.; Olaiya, B. S.; Castellano, F. N. *J. Am. Chem. Soc.* **2013**, *135*, 14068-14070.

- (22) Whang, D. R.; Sakai, K.; Park, S. Y. *Angew. Chem., Int. Ed. Engl.* **2013**, *52*, 11612-11615.
- (23) Stoll, T.; Gennari, M.; Fortage, J.; Castillo, C. E.; Rebarz, M.; Sliwa, M.; Poizat, O.; Odobel, F.; Deronzier, A.; Collomb, M.-N. *Angew. Chem., Int. Ed. Engl.* **2014**, *53*, 1654-1658.
- (24) Ceconi, B.; Manfredi, N.; Montini, T.; Fornasiero, P.; Abbotto, A. *Eur. J. Org. Chem.* **2016**, *2016*, 5194-5215.
- (25) Lazarides, T.; McCormick, T.; Du, P. W.; Luo, G. G.; Lindley, B.; Eisenberg, R. *J. Am. Chem. Soc.* **2009**, *131*, 9192-9194.
- (26) Han, Z.; McNamara, W. R.; Eum, M.-S.; Holland, P. L.; Eisenberg, R. *Angew. Chem., Int. Ed.* **2012**, *51*, 1667-1670, S1667/1661-S1667/1614.
- (27) Han, Z.; Shen, L.; Brennessel, W. W.; Holland, P. L.; Eisenberg, R. *J. Am. Chem. Soc.* **2013**, *135*, 14659-14669.
- (28) Lakadamyali, F.; Kato, M.; Muresan, N. M.; Reisner, E. *Angew. Chem. Int. Ed.* **2012**, *51*, 9381-9384.
- (29) Zheng, H.-Q.; Rao, H.; Hu, X.-Z.; Li, X.-H.; Fan, Y.-T.; Hou, H.-W. *Solar Energy* **2014**, *105*, 648-655.
- (30) Orain, C.; Quentel, F.; Gloaguen, F. *ChemSuschem* **2014**, *7*, 638-643.
- (31) Hartley, C. L.; DiRisio, R. J.; Screen, M. E.; Mayer, K. J.; McNamara, W. R. *Inorg. Chem.* **2016**, *55*, 8865-8870.
- (32) McLaughlin, M. P.; McCormick, T. M.; Eisenberg, R.; Holland, P. L. *Chem. Commun.* **2011**, *47*, 7989-7991.
- (33) Das, A.; Han, Z.; Brennessel, W. W.; Holland, P. L.; Eisenberg, R. *ACS Catal.* **2015**, *5*, 1397-1406.
- (34) Song, X.; Wen, H.; Ma, C.; Chen, H.; Chen, C. *New J. Chem.* **2015**, *39*, 1734-1741.
- (35) Rao, H.; Yu, W.-Q.; Zheng, H.-Q.; Bonin, J.; Fan, Y.-T.; Hou, H.-W. *J. Power Sources* **2016**, *324*, 253-260.
- (36) Kankanamalage, P. H. A.; Mazumder, S.; Tiwari, V.; Kpogo, K. K.; Bernhard Schlegel, H.; Verani, C. N. *Chem. Commun.* **2016**, *52*, 13357-13360.
- (37) McCormick, T. M.; Calitree, B. D.; Orchard, A.; Kraut, N. D.; Bright, F. V.; Detty, M. R.; Eisenberg, R. *J. Am. Chem. Soc.* **2010**, *132*, 15480-15483.
- (38) Gong, L.; Wang, J.; Li, H.; Wang, L.; Zhao, J.; Zhu, Z. *Catal. Commun.* **2011**, *12*, 1099-1103.
- (39) Bartelmess, J.; Francis, A. J.; El Roz, K. A.; Castellano, F. N.; Weare, W. W.; Sommer, R. D. *Inorg. Chem.* **2014**, *53*, 4527-4534.
- (40) Manton, J. C.; Long, C.; Vos, J. G.; Pryce, M. T. *PhysChemChemPhys* **2014**, *16*, 5229-5236.
- (41) Luo, G.-G.; Lu, H.; Zhang, X.-L.; Dai, J.-C.; Wu, J.-H.; Wu, J.-J. *PhysChemChemPhys* **2015**, *17*, 9716-9729.
- (42) Luo, G.-G.; Fang, K.; Wu, J.-H.; Mo, J. *Chem. Commun.* **2015**, *51*, 12361-12364.
- (43) Sabatini, R. P.; Lindley, B.; McCormick, T. M.; Lazarides, T.; Brennessel, W. W.; McCamant, D. W.; Eisenberg, R. *J. Phys. Chem. B* **2016**, *120*, 527-534.
- (44) Weingarten, A. S.; Kazantsev, R. V.; Palmer, L. C.; McClendon, M.; Koltonow, A. R.; Samuel, A. P. S.; Kiebal, D. J.; Wasielewski, M. R.; Stupp, S. I. *Nat. Chem.* **2014**, *6*, 964-970.
- (45) Weingarten, A. S.; Kazantsev, R. V.; Palmer, L. C.; Fairfield, D. J.; Koltonow, A. R.; Stupp, S. I. *J. Am. Chem. Soc.* **2015**, *137*, 15241-15246.
- (46) Goy, R.; Bertini, L.; Rudolph, T.; Lin, S.; Schulz, M.; Zampella, G.; Dietzek, B.; Schacher, F. H.; De Gioia, L.; Sakai, K.; Weigand, W. *Chem. Eur. J.* **2017**, *23*, 334-345.
- (47) Ladomenou, K.; Natali, M.; Iengo, E.; Charalampidis, G.; Scandola, F.; Coutsolelos, A. G. *Coord. Chem. Rev.* **2015**, *304-305*, 38-54.
- (48) Hagfeldt, A.; Boschloo, G.; Sun, L.; Kloo, L.; Pettersson, H. *Chem. Rev.* **2010**, *110*, 6595-6663.
- (49) Laursen, B. W.; Krebs, F. C. *Angew. Chem. Int. Ed.* **2000**, *39*, 3432-3434.
- (50) W. Laursen, B.; C. Krebs, F. *Chem. Eur. J.* **2001**, *7*, 1773-1783.
- (51) Dileesh, S.; Gopidas, K. R. *J. Photochem. Photobiol. A* **2004**, *162*, 115-120.
- (52) Bosson, J.; Gouin, J.; Lacour, J. *Chem. Soc. Rev.* **2014**, *43*, 2824-2840.
- (53) Varma, S.; Castillo, C. E.; Stoll, T.; Fortage, J.; Blackman, A. G.; Molton, F.; Deronzier, A.; Collomb, M.-N. *PhysChemChemPhys* **2013**, *15*, 17544-17552.
- (54) Gimbert-Surinach, C.; Albero, J.; Stoll, T.; Fortage, J.; Collomb, M.-N.; Deronzier, A.; Palomares, E.; Llobet, A. *J. Am. Chem. Soc.* **2014**, *136*, 7655-7661.
- (55) Gueret, R.; Castillo, C. E.; Rebarz, M.; Thomas, F.; Hargrove, A.-A.; Pécaut, J.; Sliwa, M.; Fortage, J.; Collomb, M.-N. *J. Photochem. Photobiol., B* **2015**, *152*, 82-94.
- (56) Roy, S.; Bacchi, M.; Berggren, G.; Artero, V. *ChemSuschem* **2015**, *8*, 3632-3638.
- (57) Hammershøj, P.; Sørensen, T. J.; Han, B.-H.; Laursen, B. W. *J. Org. Chem.* **2012**, *77*, 5606-5612.
- (58) Sørensen, T. J.; Hildebrandt, C. B.; Glyvradal, M.; Laursen, B. W. *Dyes Pigm.* **2013**, *98*, 297-303.
- (59) Adam, C.; Wallabregue, A.; Li, H.; Gouin, J.; Vanel, R.; Grass, S.; Bosson, J.; Bouffier, L.; Lacour, J.; Sojic, N. *Chem. Eur. J.* **2015**, *21*, 19243-19249.
- (60) Thyrhaug, E.; Sørensen, T. J.; Gryczynski, I.; Gryczynski, Z.; Laursen, B. W. *J. Phys. Chem. A* **2013**, *117*, 2160-2168.
- (61) Bogh, S. A.; Simmermacher, M.; Westberg, M.; Bregnhøj, M.; Rosenberg, M.; De Vico, L.; Veiga, M.; Laursen, B. W.; Ogilby, P. R.; Sauer, S. P. A.; Sørensen, T. J. *ACS Omega* **2017**, *2*, 193-203.
- (62) Cabrerizo, F. M.; Arbjerg, J.; Denofrio, M. P.; Erra-Balsells, R.; Ogilby, P. R. *ChemPhysChem* **2010**, *11*, 796-798.
- (63) Klonis, N.; Sawyer, W. H. *J. Fluoresc.* **1996**, *6*, 147-157.
- (64) Zhang, X.-F.; Yang, X. J. *Phys. Chem. B* **2013**, *117*, 5533-5539.
- (65) Kamat, P. V.; Fox, M. A. *J. Phys. Chem.* **1984**, *88*, 2297-2302.
- (66) Hashimoto, K.; Kawai, T.; Sakata, T. *Nouv. J. Chim.* **1984**, *8*, 393-700.
- (67) Mau, A. W. H.; Johansen, O.; Sasse, W. H. F. *Photochem. Photobiol.* **1985**, *41*, 503-509.
- (68) Duchowicz, R.; Ferrer, M. L.; Acuña, A. U. *Photochem. Photobiol.* **1998**, *68*, 494-501.
- (69) Zhang, P.; Wang, M.; Dong, J. F.; Li, X. Q.; Wang, F.; Wu, L. Z.; Sun, L. C. *J. Phys. Chem. C* **2010**, *114*, 15868-15874.
- (70) Zhang, X.-F.; Zhang, I.; Liu, L. *Photochem. Photobiol.* **2010**, *86*, 492-498.
- (71) Li, X. Q.; Wang, M.; Zheng, D. H.; Han, K.; Dong, J. F.; Sun, L. C. *Energy Environ. Sci.* **2012**, *5*, 8220-8224.
- (72) Wu, W.; Guo, H.; Wu, W.; Ji, S.; Zhao, J. *J. Org. Chem.* **2011**, *76*, 7056-7064.
- (73) Sabatini, R. P.; McCormick, T. M.; Lazarides, T.; Wilson, K. C.; Eisenberg, R.; McCamant, D. W. *J. Phys. Chem. Lett.* **2011**, *2*, 223-227.
- (74) Math, N. N.; Naik, L. R.; Suresh, H. M.; Inamdar, S. R. *J. Lumin.* **2006**, *121*, 475-487.
- (75) McCormick, T. M.; Han, Z. J.; Weinberg, D. J.; Brennessel, W. W.; Holland, P. L.; Eisenberg, R. *Inorg. Chem.* **2011**, *50*, 10660-10666.
- (76) Cui, H.-H.; Wang, J.-Y.; Hu, M.-Q.; Ma, C.-B.; Wen, H.-M.; Song, X.-W.; Chen, C.-N. *Dalton Trans.* **2013**, *42*, 8684-8691.
- (77) Rao, H.; Wang, Z.-Y.; Zheng, H.-Q.; Wang, X.-B.; Pan, C.-M.; Fan, Y.-T.; Hou, H.-W. *Catal. Sci. Technol.* **2015**, *5*, 2332.
- (78) Dong, J. F.; Wang, M.; Zhang, P.; Yang, S. Q.; Liu, J. Y.; Li, X. Q.; Sun, L. C. *J. Phys. Chem. C* **2011**, *115*, 15089-15096.
- (79) Sørensen, T. J.; Nielsen, M. F.; Laursen, B. W. *ChemPlusChem* **2014**, *79*, 1030-1035.
- (80) Bosson, J.; Labrador, G. M.; Pascal, S.; Miannay, F.-A.; Yushchenko, O.; Li, H.; Bouffier, L.; Sojic, N.; Tovar, R. C.; Muller, G.; Jacquemin, D.; Laurent, A. D.; Le Guennic, B.; Vauthey, E.; Lacour, J. *Chem. Eur. J.* **2016**, *22*, 18394-18403.

- (81) Li, H.; Voci, S.; Wallabregue, A.; Adam, C.; Labrador, G. M.; Duwald, R.; Hernández Delgado, I.; Pascal, S.; Bosson, J.; Lacour, J.; Bouffier, L.; Sojic, N. *ChemElectroChem* **2017**, 1750-1756.
- (82) Luo, G.-G.; Fang, K.; Wu, J.-H.; Dai, J.-C.; Zhao, Q.-H. *PhysChemChemPhys* **2014**, 16, 23884-23894.
- (83) Natali, M. *ACS Catal.* **2017**, 1330-1339.
- (84) Pellegrin, Y.; Odobel, F. *C. R. Chim.* **2017**, 20, 283-295.
- (85) Singh, W. M.; Baine, T.; Kudo, S.; Tian, S.; Ma, X. A. N.; Zhou, H.; DeYonker, N. J.; Pham, T. C.; Bollinger, J. C.; Baker, D. L.; Yan, B.; Webster, C. E.; Zhao, X. *Angew. Chem. Int. Ed.* **2012**, 51, 5941-5944.
- (86) Guttentag, M.; Rodenberg, A.; Bachmann, C.; Senn, A.; Hamm, P.; Alberto, R. *Dalton Trans.* **2013**, 42, 334-337.
- (87) Natali, M.; Luisa, A.; Iengo, E.; Scandola, F. *Chem. Commun.* **2014**, 50, 1842-1844.
- (88) Khnayzer, R. S.; Thoi, V. S.; Nippe, M.; King, A. E.; Jurss, J. W.; El Roz, K. A.; Long, J. R.; Chang, C. J.; Castellano, F. N. *Energy Environ. Sci.* **2014**, 7, 1477-1488.
- (89) Singh, W. M.; Mirmohades, M.; Jane, R. T.; White, T. A.; Hammarstrom, L.; Thapper, A.; Lomoth, R.; Ott, S. *Chem. Commun.* **2013**, 49, 8638-8640.
- (90) Bachmann, C.; Probst, B.; Guttentag, M.; Alberto, R. *Chem. Commun.* **2014**, 50, 6737-6739.
- (91) Deponti, E.; Luisa, A.; Natali, M.; Iengo, E.; Scandola, F. *Dalton Trans.* **2014**, 43, 16345-16353.
- (92) Vennampalli, M.; Liang, G.; Katta, L.; Webster, C. E.; Zhao, X. *Inorg. Chem.* **2014**, 53, 10094-10100.
- (93) Lo, W. K. C.; Castillo, C. E.; Gueret, R.; Fortage, J.; Rebarz, M.; Sliwa, M.; Thomas, F.; McAdam, C. J.; Jameson, G. B.; McMorran, D. A.; Crowley, J. D.; Collomb, M.-N.; Blackman, A. G. *Inorg. Chem.* **2016**, 55, 4564-4581.
- (94) Lucarini, F.; Pastore, M.; Vasylevskiy, S.; Varisco, M.; Solari, E.; Crochet, A.; Fromm, K. M.; Zobi, F.; Ruggi, A. *Chem. Eur. J.* **2017**, 23, 6768-6771.
- (95) Stoll, T.; Gennari, M.; Serrano, I.; Fortage, J.; Chauvin, J.; Odobel, F.; Rebarz, M.; Poizat, O.; Sliwa, M.; Deronzier, A.; Collomb, M.-N. *Chem. Eur. J.* **2013**, 19, 782-792.
- (96) CollombDunandSauthier, M. N.; Deronzier, A.; LeBozec, H.; Navarro, M. *J. Electroanal. Chem.* **1996**, 410, 21-29.
- (97) Guttentag, M.; Rodenberg, A.; Kopelent, R.; Probst, B.; Buchwalder, C.; Brandstätter, M.; Hamm, P.; Alberto, R. *Eur. J. Inorg. Chem.* **2012**, 2012, 59-64.
- (98) Creutz, C.; Sutin, N.; Brunshwig, B. S. *J. Am. Chem. Soc.* **1979**, 101, 1297-1298.
- (99) Bielski, B. H. J.; Allen, A. O.; Schwarz, H. A. *J. Am. Chem. Soc.* **1981**, 103, 3516-3518.
- (100) Moonshiram, D.; Gimbert-Suriñach, C.; Guda, A.; Picon, A.; Lehmann, C. S.; Zhang, X.; Doumy, G.; March, A. M.; Benet-Buchholz, J.; Soldatov, A.; Llobet, A.; Southworth, S. H. *J. Am. Chem. Soc.* **2016**, 138, 10586-10596.
- (101) Lewandowska-Andralojc, A.; Baine, T.; Zhao, X.; Muckerman, J. T.; Fujita, E.; Polyansky, D. E. *Inorg. Chem.* **2015**, 54, 4310-4321.
- (102) Castillo, C. E.; Gennari, M.; Stoll, T.; Fortage, J.; Deronzier, A.; Collomb, M. N.; Sandroni, M.; Légalité, F.; Blart, E.; Pellegrin, Y.; Delacote, C.; Boujtita, M.; Odobel, F.; Rannou, P.; Sadki, S. *J. Phys. Chem. C* **2015**, 119, 5806-5818.
- (103) Kayanuma, M.; Stoll, T.; Daniel, C.; Odobel, F.; Fortage, J.; Deronzier, A.; Collomb, M.-N. *PhysChemChemPhys* **2015**, 17, 10497-10509.
- (104) Kitamoto, K.; Sakai, K. *Angew. Chem., Int. Ed. Engl.* **2014**, 53, 4618-4622.
- (105) Kitamoto, K.; Sakai, K. *Chem. Commun.* **2016**, 52, 1385-1388.
- (106) Tsuji, Y.; Yamamoto, K.; Yamauchi, K.; Sakai, K. *Angew. Chem.* **2018**, 130, 214-218.

Graphical abstract

